First-principles study of La and Sb-doping effects on electronic structure and optical properties of $SrTiO_3$*

Yun Jiang-Ni(贠江妮)[a)b)], Zhang Zhi-Yong(张志勇)[a)†],
Yan Jun-Feng(闫军锋)[a)], and Deng Zhou-Hu(邓周虎)[a)]

[a)] *School of Information Science and Technology, Northwest University, Xi'an* 710127, *China*
[b)] *Institute of Photonics and Photon-Technology of Northwest University, Xi'an* 710069, *China*

(Received 8 May 2009; revised manuscript received 23 July 2009)

The effects of La and Sb doping on the electronic structure and optical properties of $SrTiO_3$ are investigated by first-principles calculation of the plane wave ultra-soft pseudo-potential based on density functional theory. The calculated results reveal that corner-shared TiO_6 octahedra dominate the main electronic properties of $SrTiO_3$, and its structural stability can be improved by La doping. The La^{3+} ion fully acts as an electron donor in $Sr_{0.875}La_{0.125}TiO_3$ and the Fermi level shifts into the conduction bands (CBs) after La doping. As for $SrSb_{0.125}Ti_{0.875}O_3$, there is a distortion near the bottom of the CBs for $SrSb_{0.125}Ti_{0.875}O_3$ after Sb doping and an incipient localization of some of the doped electrons trapped in the Ti site, making it impossible to describe the evolution of the density of states (DOS) within the rigid band model. At the same time, the DOSs of the two electron-doped systems shift towards low energies and the optical band gaps are broadened by about 0.4 and 0.6 eV for $Sr_{0.875}La_{0.125}TiO_3$ and $SrSb_{0.125}Ti_{0.875}O_3$, respectively. Moreover, the transmittance of $SrSb_{0.125}Ti_{0.875}O_3$ is as high as 95% in most of the visible region, which is higher than that of $Sr_{0.875}La_{0.125}TiO_3$(85%). The wide band gap, the small transition probability and the weak absorption due to the low partial density of states (PDOS) of impurity in the Fermi level result in the significant optical transparency of $SrSb_{0.125}Ti_{0.875}O_3$.

Keywords: density functional theory, $SrTiO_3$, doping, electronic structure

PACC: 7115M, 7125, 7155, 7850

1. Introduction

Exploration of materials for transparent conducting oxide (TCO) has been an urgent task because the rapid expansion of the industrial uses of TCO films in liquid crystal displays, organic light emitting diodes and solar cells.[1−3] In particular, this is compounded by the increasing potential new uses for TCO films[4−6] (e.g. the transparent field-effect transistor) and a resource problem for Sn-doped In_2O_3 (ITO),[2,3] which is a typical TCO and the most widely used.

Perovskite oxides are attractive candidates for TCO films. Recently, by ionic substitution and carrier doping, TCO films with the perovskite structure have been explored, and a few of them including La, Sb and In-doped $SrTiO_3$,[7−9] Nb-doped $CaTiO_3$,[10] Cd_3TeO_6,[11] Sb-doped $SrSnO_3$,[3] La and Sb-doped $BaSnO_3$[6] have been obtained in experiment. Wang *et al.*[7] have demonstrated that Sb-doped $SrTiO_3$ thin films epitaxially grown on $SrTiO_3$ (001) substrates by pulsed laser deposition show good optical transmittance in the visible range. Cho *et al.*[8] have found that $La_{0.5}Sr_{0.5}TiO_{3+\delta}$ thin films exhibit excellent transparent properties of visible light with a metallic behaviour. Guo *et al.*[9] have reported on the optical properties of p-type $SrIn_xTi_{1-x}O_3$ ($x = 0.1$ and 0.2) films prepared by laser molecular beam epitaxy under different oxygen pressures and the high transparence of the films in most of the visible region. To our knowledge, however, theoretical investigations on TCO films with the perovskite structure are rare. Thus it is necessary to use the first-principles method to explore the effect of carrier doping on the electronic structure and the optical property of perovskite oxides.

In the present paper, we perform a first-principles calculation to investigate the effects of n-type doping La and Sb on the perovskite oxide $SrTiO_3$ by the CASTEP software package[12] based on density functional theory (DFT). From these results, a better understanding of the electronic structure and the optical properties of La and Sb-doped $SrTiO_3$ with sufficient details can be reached, and some helpful instructions can be provided for the growth of TCO films with the perovskite structure.

*Project supported by the Northwest University (NWU) Graduate Innovation and Creativity Funds (Grant No. 08YZZ47) and the Natural Science Foundation of Shaanxi Province of China (Grant No. 2009JM8013).
†Corresponding author. E-mail: zhangzy@nwu.edu.cn
© 2010 Chinese Physical Society and IOP Publishing Ltd

2. Computational details

$SrTiO_3$ has an ideal cubic perovskite-type structure at room temperature, and it belongs to the space group $Pm3m(O_{h1})$, with the Sr atom sitting at the origin point, Ti at the body centre and three oxygen atoms at the three face centres, and its lattice constant is $a = b = c = 3.905$ Å (1 Å = 0.1 nm).[13] The unit cell contains one formula unit of $SrTiO_3$. Figure 1 shows the schematic structures of $SrTiO_3$. In order to study fractional substitution, it is necessary to consider a larger cell than the basic unit. Thus we construct a supercell of eight unit cells consisting of 40 atoms in the basis. Replacing any one of the Sr atoms by a La atom in the supercell will correspond to the formula $Sr_{0.875}La_{0.125}TiO_3$ or $Sr_{1-x}La_xTiO_3$ with $x = 0.125$. Substitution of a single Sb atom for Ti atoms will correspond to the formula $SrSb_{0.125}Ti_{0.875}O_3$.

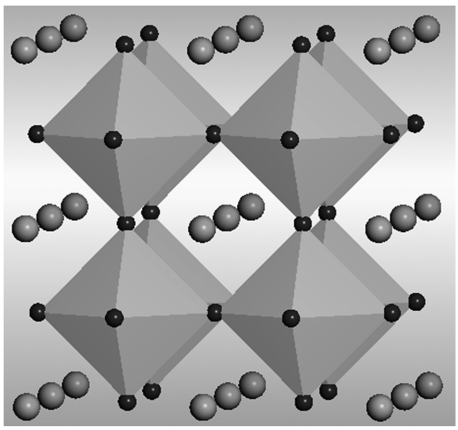


Fig. 1. Schematic crystal structure of $SrTiO_3$.

In our computation, the interaction between nuclei and electrons is approximated by using the Vanderbilt ultra-soft pseudo-potential[14] to treat 4s, 4p, and 5s electrons of Sr, 3s, 3p, 3d, and 4s electrons of Ti, 2s and 2p electrons of O, 5s and 5p electrons of Sb, and 5s, 5p, 5d, and 6s electrons of La as the valence electrons. The Perdew and Wang 91 parametrization[15] is taken as the exchange-correlation potential in the generalized-gradient approximation (GGA). A plane wave basis with kinetic energy cutoff of 420 eV is used to represent wave functions. The Brillouin zone integration is approximated as a special k-point sampling scheme of Monkhorst–Pack[16] and 6×6×6 k-point grids are used. In order to obtain a stable structure, a full relaxation is performed for doped Sr_2TiO_4 systems by using the Broyden–Fletcher–Goldfarb–Shanno (BFGS) algorithm[17] to minimize energy with respect to atomic position. Each calculation is considered to be converged when the maximum root-mean-square convergent tolerance is less than 5.0×10^{-6} eV/atom, that is, the maximum ionic Hellmann–Feynman force being within 0.01 eV/Å, the maximum ionic displacement being within 5.0×10^{-4} Å and the maximum stress being within 0.02 GPa. Then the electronic structure and optical properties are calculated based on the optimized supercell model.

3. Results and discussion

3.1. Cohesive energy and lattice properties

The cohesive intensity and the structural stability of a crystal are related to its cohesive energy, and the cohesive energy of a crystal is defined as either the energy that is needed when the crystal is formed by combining with a free atom, or the work that needs to be performed when the crystal decomposes into a single atom. Hence, the bigger the cohesive energy is, the more stable the crystal structure will be. In this paper, the cohesive energies of $SrTiO_3$, $Sr_{1-x}La_xTiO_3$ and $SrSb_xTi_{1-x}O_3$ with $x = 0.125$ are calculated from the formulas in Ref. [18]. By analysing the calculated cohesive energies listed in Table 1, we conclude that the optimized $SrTiO_3$, $Sr_{0.875}La_{0.125}TiO_3$ and $SrSb_{0.125}Ti_{0.875}O_3$ systems are stable, because the cohesive energies are negative. On the other hand, the cohesive energy of La-doped $Sr_{0.875}La_{0.125}TiO_3$ (–43.2810 eV) is smaller than that of undoped $SrTiO_3$ (–42.8037 eV), which indicates that $Sr_{0.875}La_{0.125}TiO_3$ is more stable than undoped Sr_2TiO_4 and the structural stability of $SrTiO_3$ can be improved by La doping. However, the Sb-doped $SrSb_{0.125}Ti_{0.875}O_3$ is less stable than $SrTiO_3$. Furthermore, it is clear that after doping the single point energy of $Sr_{0.875}La_{0.125}TiO_3$ decreases, which further confirms that the structural stability of $SrTiO_3$ can be strengthened by La doping, while the increasing of the single point energy of $SrSb_{0.125}Ti_{0.875}O_3$ implies that the structural stability of $SrTiO_3$ is weakened by Sb doping. These structural stability changes for $Sr_{0.875}La_{0.125}TiO_3$ and $SrSb_{0.125}Ti_{0.875}O_3$ originate from the electronic structure changes through doping, and we will discuss this later. Note that the crystal structures of $Sr_{1-x}La_xTiO_3$ and $SrSb_xTi_{1-x}O_3$ with $x = 0.125$ are still the cubic perovskite-type structure with the space group $Pm3m(O_{h1})$.

Table 1. Optimized structure parameters, single point energies (E_s) and cohesive energies (E_c) for $SrTiO_3$, $Sr_{0.875}La_{0.125}TiO_3$ and $SrSb_{0.125}Ti_{0.87}O_3$.

	space group	a/Å		E_s/eV	E_c/eV
		calculated	experimental	calculated	calculated
$SrTiO_3$	$Pm3m$	3.924	3.905[a]	–3772.466	–42.8037
$Sr_{0.875}La_{0.125}TiO_3$	$Pm3m$	3.929	3.908[b]	-3775.937	–43.2810
$SrSb_{0.125}Ti_{0.875}O_3$	$Pm3m$	3.937	3.923[c]	–3690.262	–41.7280

[a] cited from Ref. [13], [b] cited from Ref. [19], [c] cited from Ref. [7].

Moreover, the calculated lattice constant is 3.929 Å for $Sr_{0.875}La_{0.125}TiO_3$, slightly larger than that of undoped $SrTiO_3$ (3.924 Å), while the calculated lattice constant of $SrSb_{0.125}Ti_{0.875}O_3$ (3.937 Å) is much larger than that of undoped $SrTiO_3$. This is in good agreement with the experiment results[7,19] that the lattice constants of $Sr_{0.88}$ $La_{0.12}TiO_{3\pm\delta}$ and $SrSb_{0.1}Ti_{0.9}O_3$ films increase after doping.

3.2. Electronic structures

3.2.1. Density of states

In this part, the electronic structures of $SrTiO_3$, $Sr_{1-x}La_xTiO_3$ and $SrSb_xTi_{1-x}O_3$ with $x = 0.125$ will be discussed and compared with each other. Four indicators will be used to reveal the effects of La and Sb doping on the electronic structure of $SrTiO_3$, which are the total DOS, partial density of states (PDOS), population analysis, and electron density difference. Each of these tools can demonstrate some aspects of structural features. The total DOS and PDOS of $SrTiO_3$ are calculated first for comparison and the results are shown in Fig. 2. For the sake of clarity, only the relevant Ti 3d, O 2p and Sr 5p PDOS are shown and this will be adopted in the subsequent figures. It is obvious that the structure of $SrTiO_3$ has corner shared TiO_6 octahedra where the interaction between Ti 3d and O 2p is found, which dominates the main electronic properties of $SrTiO_3$. The top of the valance bands (VBs) predominantly consists of O 2p states and the most prominent unoccupied energy bands in the bottommost conduction bands (CBs) are mainly composed of the Ti 3d states. Overlooked from the DOS, it can be observed that there is a strong orbital hybridization between the Ti 3d and O 2p states. That is to say, the Ti–O bond is covalent. Correspondingly no overlap of PDOS between Sr atoms and O atoms means the high ionicity of Sr–O bonds. Moreover, the calculated band gap of $SrTiO_3$ is about 1.7 eV, which is smaller than the experimental value of about 3.2 eV.[13] This is typically underestimated by the DFT[20,21] and also caused by the strong self-interaction of the Ti 3d states.[22]

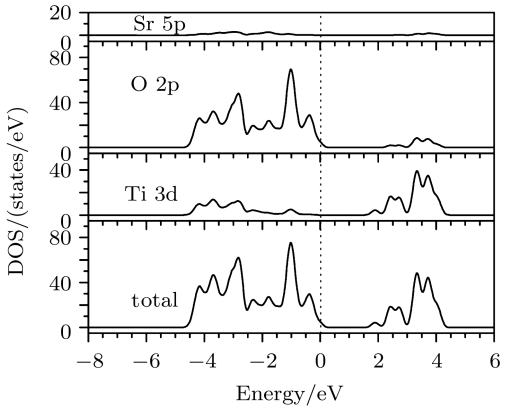


Fig. 2. DOS and PDOS of $SrTiO_3$. Fermi level is set to be zero on the energy scale, which will be adopted below unless otherwise stated.

Figure 3 shows the total DOSs of $Sr_{1-x}La_xTiO_3$ and $SrSb_xTi_{1-x}O_4$ with $x = 0.125$. Because La doping introduces n-type carriers into the $Sr_{0.875}La_{0.125}TiO_3$ system, the Fermi level shifts into the CBs, which is in good agreement with the experimental results that the La^{3+} ion fully acts as an electron donor in the $Sr_{0.90}La_{0.1}TiO_3$ system.[8,19] At the same time, the DOS of $Sr_{0.875}La_{0.125}TiO_3$ shifts significantly towards low energies and the optical band gap broadens by about 0.4 eV due to the Burstein–Moss shift.[23,24] As for the $SrSb_{0.125}Ti_{0.875}O_3$ system, it shows a further shift of the Fermi level into the CBs compared with that for $Sr_{0.875}La_{0.125}TiO_3$, and an optical band gap with a widening of 0.6 eV is observed for $SrSb_{0.125}Ti_{0.875}O_3$ after Sb doping. Thus Sb doping into $SrTiO_3$ is more effective in the expansion of the parent optical band gap.

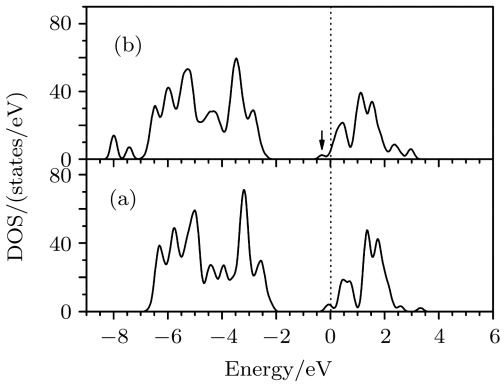


Fig. 3. DOSs of (a) $Sr_{0.875}La_{0.125}TiO_3$ and (b) $SrSb_{0.125}Ti_{0.875}O_3$.

In particular, the DOS of $Sr_{0.875}La_{0.125}TiO_3$ after La doping is almost identical to that of undoped $SrTiO_3$, indicating that the La doping effect on the electronic structure of $Sr_{0.875}La_{0.125}TiO_3$ can be fairly well described within a simple rigid band model. There is however a distortion near the bottom of CBs for $SrSb_{0.125}Ti_{0.875}O_3$ with the DOS showing a tailing to energies further below the Fermi energy (marked by arrows in Fig. 3). This is an indication of an incipient localization of some of the doped electrons trapped at the bottom of the CBs, which accords with the experiment results well,[7] and two additional small peaks appear at the bottom of the VBs for $SrSb_{0.125}Ti_{0.875}O_3$.

Furthermore, the calculated DOS at the Fermi level is about 4.96 states/eV for $SrSb_{0.125}Ti_{0.875}O_3$, which is larger than that of $Sr_{0.875}La_{0.125}TiO_3$ (3.52 states/eV). This again implies that $Sr_{0.875}La_{0.125}TiO_3$ is more stable than $SrSb_{0.125}Ti_{0.875}O_3$, which is consistent with the cohesive energy calculations.

3.2.2. Partial density of states

In the subsequent discussion on the effects of La and Sb doping on the electronic structure of $SrTiO_3$, we restrict ourselves to the states near the Fermi level, which control the physical properties of the system.

Firstly, the orbital decomposed PDOSs of La and Sb atoms in $Sr_{1-x}La_xTiO_3$ and $SrSb_xTi_{1-x}O_4$ with $x = 0.125$ are calculated and presented in Fig. 4(a). It is clear that the PDOS of the La atom in $Sr_{0.875}La_{0.125}TiO_3$ near the Fermi level is dominated by La 5d states, while Sb-derived 5s and 5p states in $SrSb_{0.125}Ti_{0.875}O_3$ do not contribute to states at the Fermi level, which suggests that La is better than Sb for n-type doping in $SrTiO_3$. Secondly, the orbital decomposed PDOSs of Ti atoms (Ti*, Ti**) near the impurity Sb in $SrSb_{0.125}Ti_{0.875}O_3$ are shown in Fig. 4(b), and the corresponding PDOS of Ti$^{\#}$atoms near the impurity La in $Sr_{0.875}La_{0.125}TiO_3$ is also plotted for comparison. In the case of $SrSb_{0.125}Ti_{0.875}O_3$, there is a strong interaction between impurity Sb and its first nearest neighbour Ti*. Especially, the 3d states of the Ti* atom near the Fermi level are strongly disturbed by the impurity charge potential due to Sb doping. With the increase of the distance between Sb and Ti atoms, the effect of the impurity charge potential on Ti** atom (the second nearest neighbour of the Sb atom) is weakened significantly and the PDOS of the Ti** atom is almost the same as that in undoped $SrTiO_3$. For La-doped $Sr_{0.875}La_{0.125}TiO_3$, the PDOS of Ti atoms near the impurity La is just identical to that of undoped $SrTiO_3$ in Fig. 1. This further confirms that the core structure of TiO_6 octahedra dominates the main electronic structure of $SrTiO_3$. Since the structure of a TiO_6 octahedron in $SrSb_{0.125}Ti_{0.875}O_3$ is changed by partial substitution of Sb for Ti, the PDOS of Ti atoms near the impurity Sb is disturbed strongly by the Sb-derived impurity charge potential, and some of the doped electrons are trapped in Ti sites. Thus the Sb doping effect on the electronic structure of $SrTiO_3$ cannot be described within the rigid band model.

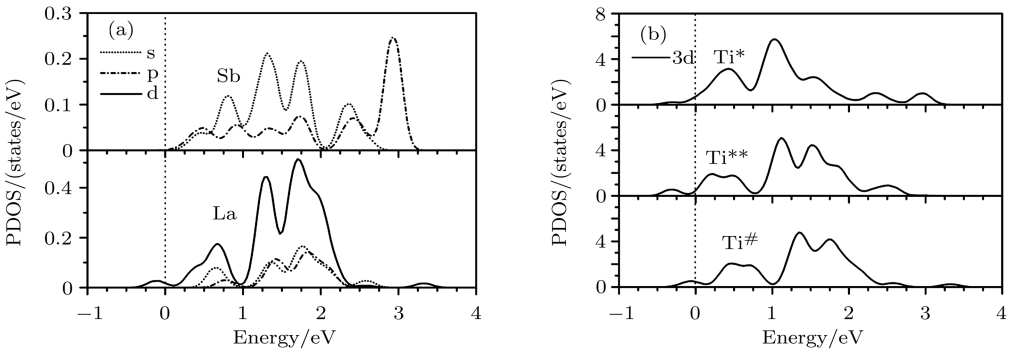


Fig. 4. Orbital decomposed PDOSs of Sb impurity and its neighbouring Ti* and Ti** atoms in $SrSb_{0.125}Ti_{0.875}O_3$; La impurity and its neighbouring Ti$^{\#}$ atom in $Sr_{0.875}La_{0.125}TiO_3$.

3.2.3. Mulliken population analysis

A further insight into the effect of La and Sb doping on the structure of $SrTiO_3$ can be obtained from Mulliken population analysis listed in Table 2. For undoped $SrTiO_3$, the effective charge of Sr (1.87e) is close to the +2e formal charges, whereas the O atom has 0.80 negative charges and the Ti atom carries 0.53 positive charges, which are much smaller than their –2e and +4e formal charges, respectively. This indicates that there is a high degree of covalency in the Ti–O bond while there is ionicity in the Sr–O bond, which accords well with the DOS analysis for $SrTiO_3$. Moreover, the calculated bond lengths of Ti–O and Sr–O bonds in $SrTiO_3$ are 1.962 and 2.771 Å, respectively, and the corresponding overlap populations are 0.62 and –0.03. These further support that the strong covalent bonding and the ionic bonding exist respectively in Ti–O and Sr–O bonds for $SrTiO_3$.

Table 2. Calculated Mulliken populations for $SrTiO_3$, $Sr_{0.875}La_{0.125}TiO_3$ and $SrSb_{0.125}Ti_{0.87}O_3$, where Ti* and O* represent the atoms near the impurity Sb atom in $SrSb_{0.125}Ti_{0.87}O_3$.

atomic population					
$SrTiO_3$		$Sr_{0.875}La_{0.125}TiO_3$		$SrSb_{0.125}Ti_{0.87}O_3$	
ion	charge/e	ion	charge/e	ion	charge/e
Sr	1.87	Sr	1.88	Sr	1.88
Ti	0.53	Ti	0.54	Ti	0.54
O	–0.80	O	–0.79	O	–0.80
		La	1.29	Sb	1.48
-	-	-	-	Ti*	0.50
-	-	-	-	O*	–0.92

bond population								
$SrTiO_3$			$Sr_{0.875}La_{0.125}TiO_3$			$SrSb_{0.125}Ti_{0.87}O_3$		
bond	population	length/Å	bond	population	length/Å	bond	population	length/Å
Sr–O	–0.03	2.771	Sr–O	–0.03	2.773	Sr–O	–0.04	2.779
Ti–O	0.62	1.962	Ti–O	0.62	1.965	Ti–O	0.63	1.958
-	-	-	La–O	0.04	2.737	Ti*–O*	0.49	1.979
-	-	-	-	-	-	Sb-O	0.54	1.948

In the case of $Sr_{0.875}La_{0.125}TiO_3$, the effective charges of Sr, Ti and O atoms in $Sr_{0.875}La_{0.125}TiO_3$ are almost the same as those in $SrTiO_3$. However, the La atom loses only partial valence electrons with 1.29e positive charges, much smaller than that of the Sr atom (1.88e). On the other hand, the overlap population values of Sr–O and Ti–O bonds do not differ from those of undoped $SrTiO_3$, and their bond lengths are slightly larger than the corresponding ones in undoped $SrTiO_3$. At the same time, a positive overlap population value of 0.04 is observed for the La–O bond in $Sr_{0.875}La_{0.125}TiO_3$ and the bond length of La–O is 2.737 Å, about 0.034 Å smaller than the Sr–O bond length in undoped $SrTiO_3$, which clearly indicates the existence of a strong interaction between the La–O bonds in $Sr_{0.875}La_{0.125}TiO_3$. Thus, the structural stability change for $Sr_{0.875}La_{0.125}TiO_3$ originates from the fact that the strength of the La–O bond is stronger than that of the Sr–O bond in undoped $SrTiO_3$.

As for $SrSb_{0.125}Ti_{0.875}O_3$, there are considerable electron charge density redistributions near the Sb atom, because the partial substitution of the Sb atom for Ti atoms has broken the TiO_6 octahedron in $SrTiO_3$. It is evident that the effective charges of O* and Ti* atoms, which are close to the impurity Sb atom, increase and decrease to values of –0.92e and 0.50e, respectively. This indicates that the electron charge densities of O* and Ti* each have some change after Sb doping. Definitely, the evidence for the electron redistribution of Ti* atoms has been given by the PDOS in Fig. 4. In particular, the value of overlap population of the Ti*–O* bond decreases to 0.49, indicating that the Ti*–O* bond is much weaker than the Ti–O bond in undoped $SrTiO_3$. The bond length of Ti*–O* is about 0.017 Å larger than that of the Ti–O bond in undoped $SrTiO_3$. Hence, judging from the changes in the M–O bonds (M = Sr, Sb, Ti) observed for $SrSb_{0.125}Ti_{0.875}O_3$, the weak Ti*–

O* bond results in the structural stability change of $SrSb_{0.125}Ti_{0.875}O_3$.

3.2.4. Electron density difference

Figure 5 plots the maps of electron density difference for $SrTiO_3$, $Sr_{0.875}La_{0.125}TiO_3$ and $SrSb_{0.125}Ti_{0.875}O_3$. For undoped $SrTiO_3$, it is clear that there is a strong covalency between Ti–O bonds and the electron cloud near the Ti and O atoms indicates the orientation characteristic of covalency, while the Sr–O bonds are quite ionic.

After La doping, the maps of doped and undoped electron density difference are almost the same. For $SrSb_{0.125}Ti_{0.875}O_3$, however, the maps of electron density difference in the (001) plane demonstrate a considerable electron charge density redistribution near the impurity Sb atom. The Sb–O bond shows covalent interaction but some ionicity. At the same time, the overlap of electron density between Ti and O atoms near the Sb atom shows a prominently weaker covalent bonding effect than the corresponding one in undoped $SrTiO_3$. Also, the electron cloud of O atoms near the Sb atom has a small distortion. This is consistent with the calculated DOS, PDOS and population analysis.

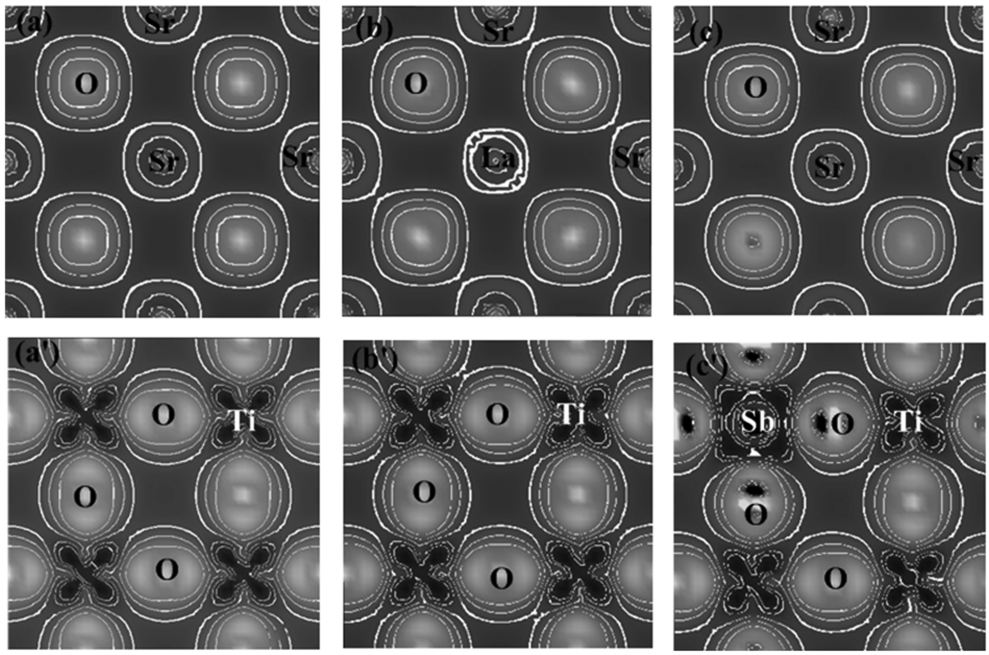


Fig. 5. Maps of electron density difference for undoped and doped $SrTiO_3$. Panels (a), (b) and (c) are the (010) planes for undoped, La-doped and Sb-doped $SrTiO_3$, respectively; panels (a'), (b') and (c') are the corresponding (001) planes.

3.3. Optical properties

Next we discuss the effects of La and Sb doping on the optical properties of $SrTiO_3$. The linear response of a system due to an external electromagnetic field with a small wave vector can be described with the complex dielectric function $\varepsilon(\omega) = \varepsilon_1(\omega) + \mathrm{i}\varepsilon_2(\omega)$. The imaginary part of the dielectric function $\varepsilon_2(\omega)$ is calculated from the momentum matrix elements between the occupied and unoccupied wave functions[25] as follows:

$$\varepsilon_2(\omega) = \frac{Ve^2}{2\pi\hbar m^2\omega^2}\int \mathrm{d}^3k \sum_{n,n'} \langle kn|p|kn'\rangle|^2 f(kn) \times(1-f(kn'))\delta(E_{kn}-E_{kn'}-\hbar\omega), \quad (1)$$

where $\hbar\omega$ is the energy of the incident photon, V is the unit cell volume, p is the momentum operator, $|kn\rangle$ is a crystal wavefunction, and $f(kn)$ is the Fermi distribution function. The real part of the dielectric function $\varepsilon_1(\omega)$ is evaluated from the imaginary part

$\varepsilon_2(\omega)$ by the Kramers–Kronig relationship to be

$$\varepsilon_1(\omega) = 1 + \frac{2}{\pi} M \int_0^{\infty} \frac{\varepsilon_2(\omega')\omega'}{\omega'^2 - \omega^2} \mathrm{d}\omega, \tag{2}$$

where M is the principal value of the integral. The other optical constants like refractive index $n(\omega)$, extinction coefficient $k(\omega)$, reflectivity $R(\omega)$ and absorption coefficient $I(\omega)$ are now immediately calculated in terms of the components of the complex dielectric function as follows:

$$n(\omega) = \left(\frac{1}{\sqrt{2}} \left[\sqrt{\varepsilon_1(\omega)^2 + \varepsilon_2(\omega)^2} + \varepsilon_1(\omega) \right] \right)^{1/2}, \tag{3}$$

$$k(\omega) = \left(\frac{1}{\sqrt{2}} \left[\sqrt{\varepsilon_1(\omega)^2 + \varepsilon_2(\omega)^2} - \varepsilon_1(\omega) \right] \right)^{1/2}, \tag{4}$$

$$R = \frac{(n-1)^2 + k^2}{(n+1)^2 + k^2}, \tag{5}$$

$$I = \frac{2K\omega}{c}. \tag{6}$$

Accordingly the transmittance $T(\omega)$ can be obtained by the following equation:

$$T(\omega) = 1 - R(\omega) - I(\omega). \tag{7}$$

Figure 6 shows optical transmittances of $Sr_{0.875}La_{0.125}TiO_3$ and $SrSb_{0.125}Ti_{0.875}O_3$. The optical transmittances of the two compounds in the visible range show that they are approximately flat curves versus wavelength. The $Sr_{0.875}La_{0.125}TiO_3$ is highly transparent with a transmittance of more than 85% in the visible range. The transmittance of $SrSb_{0.125}Ti_{0.875}O_3$ is as high as 95% in most of the visible region. The significant high transparency of $SrSb_{0.125}Ti_{0.875}O_3$ originates from two factors.

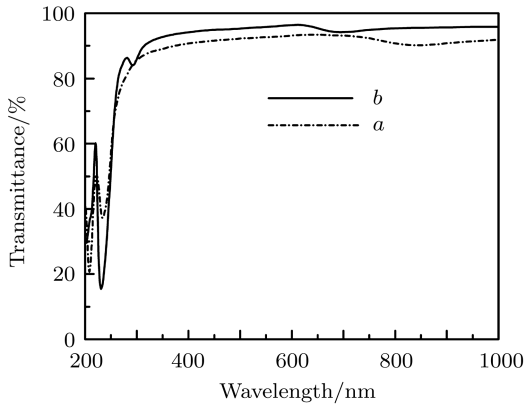


Fig. 6. Calculated optical transmittances of (a) $Sr_{0.875}La_{0.125}TiO_3$ and (b) $SrSb_{0.125}Ti_{0.875}O_3$.

On the one hand, due to being optically transparent, it is desirable to have a wider band gap than the photon energy of the visible light. It is evident that Sb doping is very effective in the expansion of the parent optical band gap (3.2 eV) and an optical band gap widening of 0.6 eV has been observed in $SrSb_{0.125}Ti_{0.875}O_3$. Thus the charge transfer excitation occurring above 3.8 eV in $SrSb_{0.125}Ti_{0.875}O_3$ benefits the optical transparency. On the other hand, the PDOS of the impurity Sb atom is low in the Fermi level (see Fig. 4), which leads to a small transition probability and weak absorption.

4. Conclusions

We investigate the structural stabilities, electronic structures, and optical transmittances of La and Sb-doped $SrTiO_3$ by a first-principles calculation of the plane wave ultra-soft pseudo-potential based on DFT. The calculated results reveal that corner shared TiO_6 octahedra dominate the main electronic properties of $SrTiO_3$. The binding energies of $SrTiO_3$, $Sr_{0.875}La_{0.125}TiO_3$ and $SrSb_{0.125}Ti_{0.875}O_3$ estimated from the electronic structure calculations indicate that the structural stability of $SrTiO_3$ can be improved by La doping. The structure of $SrSb_{0.125}Ti_{0.875}O_3$ is still stable after Sb doping, but its stability is lower than that of undoped $SrTiO_3$. The La^{3+} ion fully acts as an electron donor in $Sr_{0.875}La_{0.125}TiO_3$ and the Fermi level shifts into the CBs after La doping. As for $SrSb_{0.125}Ti_{0.875}O_3$, it shows a further shift of the Fermi level into the CBs compared with $Sr_{0.875}La_{0.125}TiO_3$. At the same time, the DOSs of the two electron-doped systems shift towards low energies and the optical band gaps are broadened by about 0.4 and 0.6 eV for $Sr_{0.875}La_{0.125}TiO_3$ and $SrSb_{0.125}Ti_{0.875}O_3$, respectively. Particularly, there is a distortion near the bottom of the CBs for $SrSb_{0.125}Ti_{0.875}O_3$ after Sb doping and an incipient localization of some of the doped electrons trapped in the Ti site, making it impossible to describe the evolution of the DOS within the rigid band model. Moreover, the transmittance of $SrSb_{0.125}Ti_{0.875}O_3$ is as high as 95% in most of the visible region, which is larger than that of $Sr_{0.875}La_{0.125}TiO_3$(85%). The wide band gap, small transition probability and weak absorption due to the low PDOS of impurity in the Fermi level result in the significant optical transparency of $SrSb_{0.125}Ti_{0.875}O_3$. The La and Sb-doped $SrTiO_3$ can be attractive as new TCOs with the perovskite structure, and are promising for use in perovskite transparent devices.

References

[1] Kim H and Pique A 2004 *Appl. Phys. Lett.* **84** 218

[2] Furubayashi Y, Yamada N, Hirose Y, Yamamoto Y, Otani M, Hitosugi T, Shimada T and Hasegawa T 2007 *J. Appl. Phys.* **101** 093705

[3] Liu Q Z, Wang H F, Chen F and Wu W 2008 *J. Appl. Phys.* **103** 093709

[4] Kwon Y, Li Y, Heo Y W, Jones M, Holloway P H, Norton D P, Park Z V and Li S 2004 *Appl. Phys. Lett.* **84** 2685

[5] Siddiqui J, Cagin E, Chen D and Phillips J D 2006 *Appl. Phys. Lett.* **88** 212903

[6] Wang H F, Liu Q Z, Chen F, Gao G Y, Wu W and Chen X H 2007 *J. Appl. Phys.* **101** 106105

[7] Wang H H, Chen F, Dai S Y, Zhao T, Lu H B, Cui D F, Zhou Y L, Chen Z H and Yang G Z 2001 *Appl. Phys. Lett.* **78** 1676

[8] Cho J H and Cho H J 2001 *Appl. Phys. Lett.* **79** 1426

[9] Guo H Z, Liu L F, Fei Y Y, Xiang W F, Lu H B, Dai S Y, Zhou Y L and Chen Z H 2003 *J. Appl. Phys.* **94** 4558

[10] Wang R P and Tao C J 2002 *J. Cryst. Growth* **245** 63

[11] Tetsuka H, Shan Y J, Tezuka K and Imoto H 2006 *Solid State Commun.* **137** 345

[12] Segall M D, Lindan P J D, Probert M J, Pickard C J, Hasnip P J, Clark S J and Payne M C 2002 *J. Phys. Conds. Matt.* **14** 2717

[13] Van Benthem K, Elsassser C and French R H 2001 *J. Appl. Phys.* **90** 6156

[14] Vanderbilt D 1990 *Phys. Rev.* B **41** 7892

[15] Perdew J P, Chevary J A, Vosko S H, Jackson K A, Pederson M R, Singh D J and Fiolhais C 1992 *Phys. Rev.* B **46** 6671

[16] Monkhorst H J and Pack J D 1976 *Phys. Rev.* B **13** 5188

[17] Pfrommer B G, Cote M, Louie S G and Cohen M L 1997 *J. Comput. Phys.* **131** 233

[18] Xiao B, Feng J, Zhou C T, Xing J D, Xie X J and Chen Y H 2008 *Chem. Phys. Lett.* **459** 129

[19] Hashimoto S, Kindermann L, Poulsen F W and Mogensen M 2005 *J. Alloy. Compd.* **397** 245

[20] Yang Y T, Wu J, Cai Y R, Ding R X, Song J X and Shi L C 2008 *Acta Phys. Sin.* **57** 7151 (in Chinese)

[21] Jones R O and Gunnarsson O 1989 *Rev. Mod. Phys.* **61** 689

[22] Wei S H and Zunger A 1988 *Phys. Rev.* B **37** 8958

[23] Burstein E 1954 *Phys. Rev.* **93** 632

[24] San H S, Li B, Feng B X, He Y Y and Chen C 2005 *Acta Phys. Sin.* **54** 842 (in Chinese)

[25] Saha S, Sinha T P and Mookerjee A 2000 *Phys. Rev.* B **62** 8828